




Prefrontal Cortical Connectivity Mediates Locus Coeruleus Noradrenergic Regulation of Inhibitory Control in Older Adults

Alessandro Tomassini,^{1*} Frank H. Hezemans,^{1,2*} Rong Ye,²  Kamen A. Tsvetanov,^{2,3}  Noham Wolpe,^{1,2} and  James B. Rowe^{1,2}

¹Medical Research Council Cognition and Brain Sciences Unit, University of Cambridge, Cambridge CB27EF, United Kingdom, ²Department of Clinical Neuroscience and Cambridge University Hospitals National health service Trust, University of Cambridge, Cambridge CB20QQ, United Kingdom, and ³Centre for Speech, Language and the Brain, Department of Psychology, University of Cambridge, Cambridge CB3EB, United Kingdom

Response inhibition is a core executive function enabling adaptive behavior in dynamic environments. Human and animal models indicate that inhibitory control and control networks are modulated by noradrenaline, arising from the locus coeruleus. The integrity (i.e., cellular density) of the locus coeruleus noradrenergic system can be estimated from magnetization transfer (MT)-sensitive magnetic resonance imaging (MRI), in view of neuromelanin present in noradrenergic neurons of older adults. Noradrenergic psychopharmacological studies indicate noradrenergic modulation of prefrontal and frontostriatal stopping-circuits in association with behavioral change. Here, we test the noradrenergic hypothesis of inhibitory control, in healthy adults. We predicted that locus coeruleus integrity is associated with age-adjusted variance in response inhibition, mediated by changes in connectivity between frontal inhibitory control regions. In a preregistered analysis, we used MT MRI images from $N=63$ healthy humans aged above 50 years (of either sex) who performed a Stop-Signal Task (SST), with atlas-based measurement of locus coeruleus contrast. We confirm that better response inhibition is correlated with locus coeruleus integrity and stronger connectivity between presupplementary motor area (preSMA) and right inferior frontal gyrus (rIFG), but not volumes of the prefrontal cortical regions. We confirmed a significant role of prefrontal connectivity in mediating the effect of individual differences in the locus coeruleus on behavior, where this effect was moderated by age, over and above adjustment for the mean effects of age. Our results support the hypothesis that in normal populations, as in clinical settings, the locus coeruleus noradrenergic system regulates inhibitory control.

Key words: functional connectivity; healthy ageing; locus coeruleus; neuromelanin; response inhibition; stop-signal task

Significance Statement

We show that the integrity of the locus coeruleus, the principal source of cortical noradrenaline, is related to the efficiency of response inhibition in healthy older adults. This effect is in part mediated by its effect on functional connectivity in a prefrontal cortical stopping-network. The behavioral effect, and its mediation by connectivity, are moderated by age. This supports the psychopharmacological and genetic evidence for the noradrenergic regulation of behavioral control, in a population-based normative cohort. Noradrenergic treatment strategies may be effective to improve behavioral control in impulsive clinical populations, but age, and locus coeruleus integrity, are likely to be important stratification factors.

Received June 30, 2021; revised Jan. 7, 2022; accepted Feb. 7, 2022.

Author contributions: A.T. and J.B.R. designed research; A.T. performed research; A.T., F.H.H., R.Y., and K.A.T. analyzed data; A.T. wrote the first draft of the paper; A.T., F.H.H., R.Y., K.A.T., N.W., and J.B.R. edited the paper; A.T., F.H.H., R.Y., and J.B.R. wrote the paper.

This work was supported by the Medical Research Council Intramural Grant SUAG/051 R101400 and the Wellcome Trust Grant 220258 (to J.B.R.). K.A.T. was supported by the Guarantors of Brain Grant G101149. Data collection and sharing for this project was provided by Cam-CAN (www.cam-can.org). Cam-CAN funding was provided by the United Kingdom Biotechnology and Biological Sciences Research Council Grant BB/H008217/1, together with support from the United Kingdom Medical Research Council and the University of Cambridge.

*A.T. and F.H.H. shared first authorship.

The authors declare no competing financial interests.

Correspondence should be addressed to Alessandro Tomassini at alessandro.tomassini@gmail.com.

<https://doi.org/10.1523/JNEUROSCI.1361-21.2022>

Copyright © 2022 Tomassini et al.

This is an open-access article distributed under the terms of the Creative Commons Attribution 4.0 International license, which permits unrestricted use, distribution and reproduction in any medium provided that the original work is properly attributed.

Introduction

Response inhibition underpins the control of everyday behavior, and is impaired in many neurologic and psychiatric disorders (Passamonti et al., 2018). There is converging evidence from animal models (Eagle and Baunez, 2010; Bari et al., 2011) and human psychopharmacology (Chamberlain et al., 2006, 2009), that the noradrenergic system facilitates inhibitory control for action cancellation. A prefrontal cortical network is also implicated in such response inhibition, including the right inferior frontal gyrus (rIFG) and presupplementary motor area (preSMA; Chambers et al., 2006; Duann et al., 2009; Forstmann et al., 2012; Rae et al., 2015).

Cerebral noradrenergic innervation arises from the locus coeruleus, in the brainstem. By exploiting the accumulation

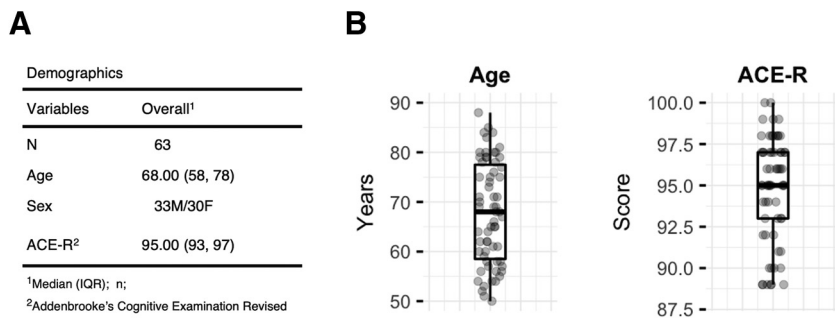


Figure 1. Demographics table (**A**) and distribution of participants' age and cognitive scores (**B**). ACE-R, Addenbrooke's Cognitive Examination Revised. The boxplots display the minimum, the maximum, the sample median, and the first and third quartiles. Dots indicate individual data.

of iron-rich neuromelanin, magnetization transfer (MT)-sensitive magnetic resonance imaging (MRI) can be used to assess the integrity of the locus coeruleus (Liu et al., 2019; Ye et al., 2021b; but see also Watanabe et al., 2019). Such studies have associated locus coeruleus integrity with diverse cognitive functions in health (Liu et al., 2020) and disease (Holland et al., 2021). Phasic and tonic activities in the locus coeruleus have been proposed to afford behavioral flexibility and inhibitory control (Aston-Jones and Cohen, 2005; Bouret and Sara, 2005; Dayan and Yu, 2006). This might be achieved by modulation of connectivity within the prefrontal network (Chambers et al., 2006; Duann et al., 2009; Forstmann et al., 2012; Ye et al., 2014; Rae et al., 2016). Here, we tested this hypothesis by linking locus coeruleus integrity to functional connectivity between rIFG and preSMA, as a predictor of behavior.

Previous analysis of cortical connectivity in healthy adults showed that the influence of cortical connectivity on inhibitory control differs with age, such that efficient performance in older adults relies more strongly on connectivity than in their younger counterparts (Tsvetanov et al., 2018).

Moreover, subregions of the locus coeruleus have different projection distributions (Mason and Fibiger, 1979; Loughlin et al., 1986) with differential associations to cognition, behavior and pathology. For example, *in vivo* evidence suggests greater degeneration of the caudal subregion of the locus coeruleus compared with middle and rostral subregions in Parkinson's disease (O'Callaghan et al., 2021). Healthy aging and age-related cognitive decline are more strongly associated with changes in the rostral locus coeruleus (Betts et al., 2017; Dahl et al., 2019).

We hypothesized that variations in the locus coeruleus integrity drive noradrenergic-dependent changes in inhibitory control, over and above the main effect of age on the locus coeruleus. We tested whether such relationship would vary across locus coeruleus subregions and across different ages. In this preregistered cross-sectional study, we used a 3D MT-weighted MRI sequence to assess the relationship between locus coeruleus integrity *in vivo* and test its relationship with inhibitory control in cognitively normal healthy adults from the Cambridge Centre for Ageing and Neuroscience cohort (Cam-CAN; Shafto et al., 2014) using the Stop-Signal Task (SST).

Our study has four main advances with respect to an earlier analysis of the Cam-CAN cohort (Liu et al., 2020). First, we use an atlas-based segmentation of the locus coeruleus, which provides unbiased estimation, with good accuracy and reliability compared with manual and semi-automatic segmentation approaches (Ye et al., 2021a). Second, we focus on middle-aged and older healthy adults, because neuromelanin accumulates

with age (Zecca et al., 2004) and in younger participants the locus coeruleus neurons may not yet be sufficiently pigmented to allow reliable inference on structural integrity by MT-weighted MRI. Third, we follow the new consensus recommendations for estimating the stop-signal reaction time (SSRT; Verbruggen et al., 2019), and use hierarchical Bayesian estimation of a parametric ex-Gaussian race model of the SST which enables isolating attentional confounds from the estimation of SSRTs (Matzke et al., 2013). Fourth, we examine whether locus coeruleus integrity is related to modulation of connectivity within the prefrontal stopping-network quantified by psychophysical interactions measures that reflect response inhibition-related changes in the connectivity between different areas (Friston et al., 1997; Tsvetanov et al., 2018).

Materials and Methods

Preregistration

Before data analysis, we preregistered our analyses, sample size, variables of interest, hypotheses, procedures for data quality checking and data analysis procedures in the Open Science Framework. The preregistered information, code and data to reproduce manuscript figures are available through the Open Science Framework (<https://osf.io/zgj9n/>).

Participants

We used data from the "Stage 3" cohort in the Cambridge Centre for Ageing and Neuroscience (Cam-CAN) population-based study of the healthy adult life span (for details, see Shafto et al., 2014). Within this cohort, we focused on 114 participants (18–88years) who performed a SST during functional MRI (fMRI). None of the Cam-CAN participants had a diagnosis of dementia or mild cognitive impairment, and all scored above consensus thresholds for normal cognition on the Addenbrooke's Cognitive Examination Revised (ACE-R >88/100). We assessed the quality of the coregistration procedure and excluded one participant because of excessive head movements (assessed by visual inspection) during the structural MRI scan session. Further, we confirmed that all included participants complied with the task, ensuring that accuracy of the 2AFC task (i.e., discriminating left vs right arrows) was above chance and the proportion of commission errors [i.e., $p(\text{response}|\text{signal})$] was between 0.25 and 0.75 following consensus guidelines (Verbruggen et al., 2019). After quality control of behavioral data and MRI scans, there were 63 datasets from participants aged 50 years or older (for details, see Fig. 1). Note that our primary statistical inferences are Bayesian, where inferences are based on relative evidence for alternate models, rather than testing a null hypothesis alone. However, for secondary frequentist statistics where Type I or Type II error may arise, we computed the achieved power using G*Power 3.1. With a nominal α level = 0.05, $N = 63$ provides 86% power to test the interaction (moderation) term of a multiple linear regression with five predictors, assuming a medium-sized effect ($f^2 = 0.15$).

Procedure

The SST assesses cognitive control systems involved in action cancellation using stop-signal trials ($n = 80$; ~50% of which were successful), randomly interleaved among go trials ($n = 360$) and no-go trials ($n = 40$) during two consecutive scanning runs (Fig. 2A). On go trials participants saw a black arrow (duration 1000ms) and indicated its direction by pressing left or right buttons with the index or middle finger of their right hand. On stop-signal trials, the black arrow changed color (from black to red) concurrent with a tone, after a short, variable "stop-signal" delay (SSD). On no-go trials, the arrow was red from the outset (i.e., SSD = 0), along with a concurrent equivalent tone. Participants were

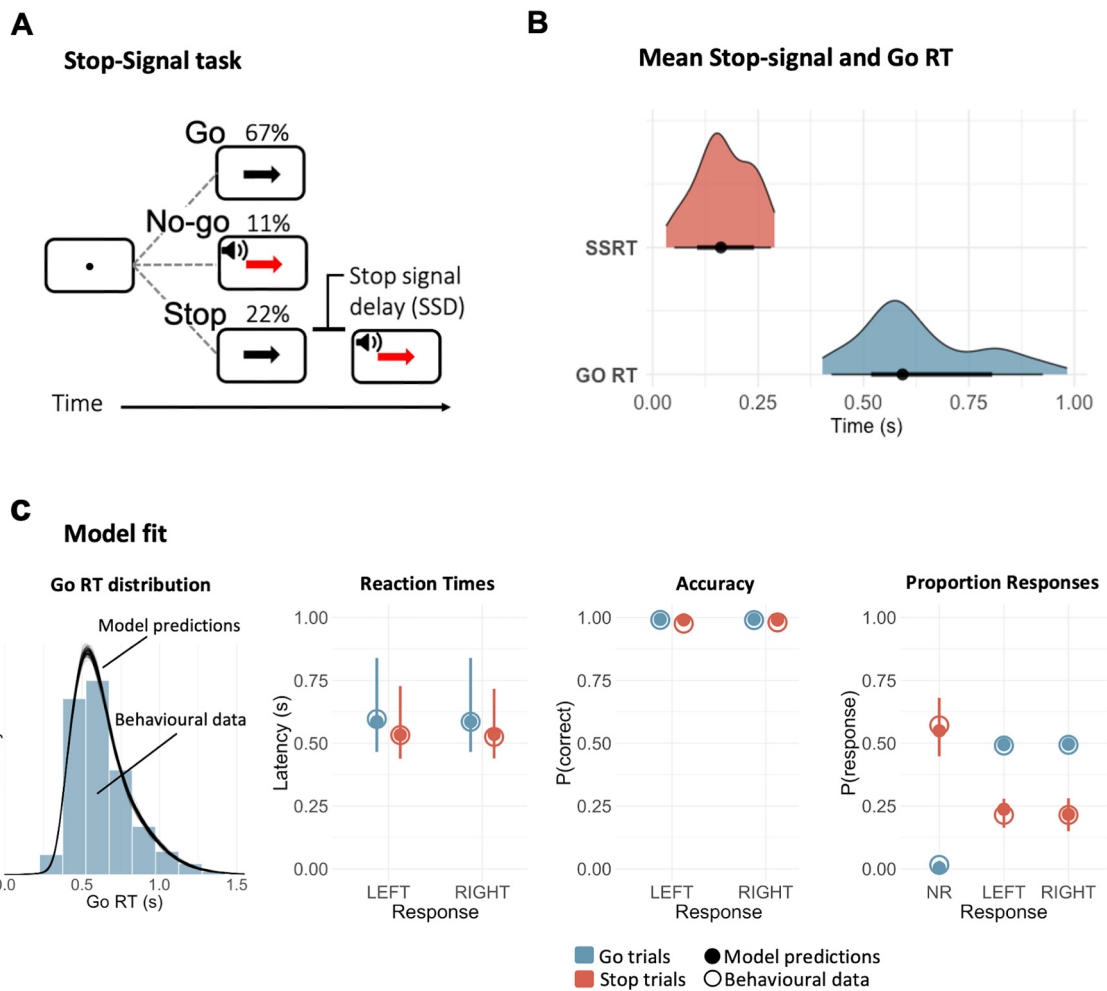


Figure 2. SST (**A**) and SSRTs estimated by the ex-Gaussian race model of response inhibition (**B**). **A**, In the SST, participants respond to the direction of a black arrow by pressing the corresponding key as accurately and as quickly as possible. Occasionally, a red arrow and a tone (stop signal) require the participants to inhibit their response. The stop signal could either appear immediately after the fixation point (no-go trials) or after a short delay (SSD) that varies across trials. **B**, Distributions of mean SSRT and go RT. The ex-Gaussian race model depicts task performance as a race between a stop process and a go process. Successful inhibition in stop and no-go trials occurs when the stop process finishes its race before the go process. The black circles indicate the medians, the thick black segments depict the 66% quantile intervals, and the thin black segments depict the 95% quantile interval. **C**, Posterior predictive checks: comparing empirical data to simulated results from the fitted model. The first panel shows histograms of the observed Go RT distributions. The black lines show 1000 Go RT distributions predicted by the model. Within each of the other panels, the group-level median values are plotted separately for each response (left, right and NR, no response, when applicable) and trial type (go, stop). Please note that for reaction times and accuracy, responses in stop trials correspond to commission errors, whereas for Proportion Responses, no response in go trials are omission errors. Model predictions are represented by the median (filled circles) and 95% quantile intervals (error bars) of 100 simulated participants, randomly drawn from the joint posterior distribution.

instructed to withhold button pressing if the arrow was red or became red. The length of the SSD varied between stop-signal trials in steps of 50 ms and was titrated to participants' performance using an on-line tracking algorithm to target a 50% successful response cancellation. No-go trials were included as stop trials with nominal SSD = 5 ms (Matzke et al., 2019).

Imaging

Imaging data were acquired with a 3T Siemens TIM trio with a 32-channel head coil. For each participant, a 3D structural MRI was acquired using a T1-weighted sequence with generalized autocalibrating partially parallel acquisition. The adopted parameters were as follows: acceleration factor, 2; repetition time (TR) = 2250 ms; echo time (TE) = 2.99 ms; inversion time = 900 ms; flip angle = 9°; field of view (FOV) = 256 × 240 × 192 mm; resolution = 1 mm isotropic.

For fMRI, echoplanar imaging (EPI) captured 32 slices in sequential descending order with slice thickness of 3.7 mm and a slice gap of 20% for whole-brain coverage. The adopted parameters were as follows: TR = 2000 ms; TE = 30 ms; flip angle = 78°; FOV = 192 × 192 mm; resolution = 3 × 3 × 4.4 mm, with a total duration of ~10 min 30 s. For preprocessing details, see Taylor et al. (2017).

MT-weighted images for each participant were obtained from a 3D, MT-prepared spoiled gradient echo sequence with either TR = 30 ms or TR = 50 ms (depending on whether the participant's SAR estimation for the TR = 30 ms sequences exceeded the stimulation limits); TE = 5 ms; flip angle = 12°; FOV = 192 × 192 mm; resolution = 1.5 mm isotropic; bandwidth = 190 Hz/px; acquisition time = 2 min 36 s per sequence for TR = 30 ms, and 4 min 19 s per sequence for TR = 50 ms. A Gaussian shaped RF pulse with an offset frequency of 1950 Hz (bandwidth = 375 Hz, 500° flip angle, duration = 9984 μs) was used for MT-weighting. MT-weighted and T1-weighted images were then processed and analyzed as described in the following.

Image processing followed a co-registration pipeline similar to Ye et al. (2021b), with Advanced Normalization Tools (ANTs v2.2.0) software and in-house MATLAB scripts. MT images were N4 bias field corrected for spatial inhomogeneity (number of iterations at each resolution level: 50 × 50 × 30 × 20, convergence threshold: 1×10^{-6} , isotropic sizing for b-spline fitting: 200) and to skull-strip T1-w images after segmentation and reconstruction (SPM12 v7219; www.fil.ion.ucl.ac.uk/spm/software/spm12). The resulting T1-w and preprocessed MT-weighted images were entered into a T1-driven, cross-modality co-registration pipeline to warp the individual MT and MT-off images to the isotropic 0.5-mm

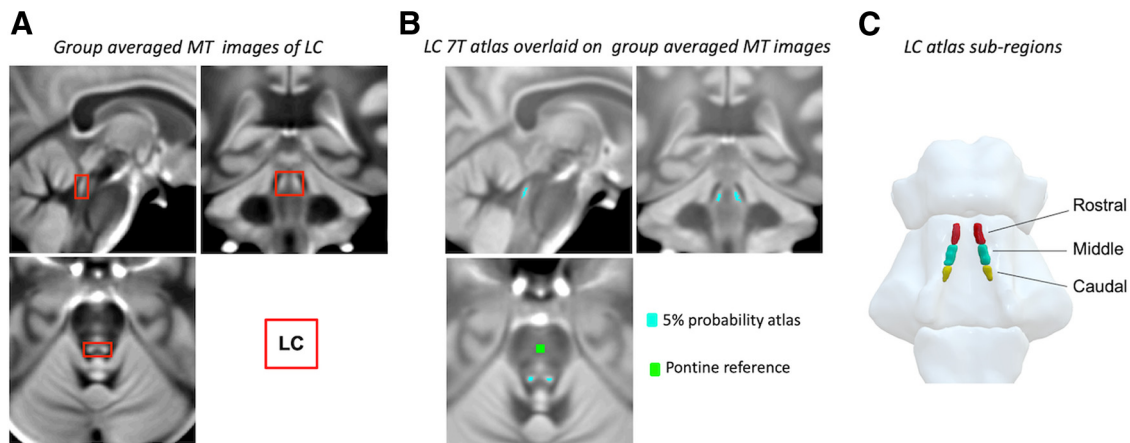


Figure 3. *A*, Sagittal, coronal, transversal view (clockwise) of group-averaged MT images. On each image the locus coeruleus (LC) is highlighted by a red square. *B*, Study-specific atlas of the LC (light blue, threshold 5%) and reference region in the central pons (green). *C*, Probabilistic LC maps thresholded at 5% presented in a 3D-reconstructed brainstem and segregated in three subregions (equal number of z slices).

ICBM152 (International Consortium for Brain Mapping) T1-w asymmetric template.

We created an unbiased study-specific T1-w structural template using individual skull-stripped T1-w images from all participants (Fig. 3A). Native T1-w images were first rigid and affine transformed, and then processed with a hierarchical nonlinear diffeomorphic step at five levels of resolution, repeated by six runs to improve convergence. The resulting T1-w group template was then registered to the standard ICBM152 T1-w brain. Four steps of deformations were estimated in the following order: MT-off to MT, T1-w to MT-off, T1-w to T1-w group template and T1-w group template to ICBM152 T1-w template. The resulting parameters were used as the roadmap for MT image standardization to the ICBM brain in one step. For co-registration details, see Ye et al. (2021b).

To facilitate accurate extraction of the locus coeruleus signal we adopted a probabilistic locus coeruleus atlas (Ye et al., 2021b) generated from ultra-high field 7T MRI of healthy adults aged 50 years and above, accompanied by a multi-modality co-registration pipeline. Voxels were categorized as lying within the locus coeruleus if their intensities were greater than the mean intensity of the reference region ($Mean_{REF}$) by >5 standard deviations (SD_{REF}). A probabilistic atlas was created by adding and averaging the individual locus coeruleus binary mask segmented from the previous thresholding step. This yielded a map covering the spatial extent of the structure at the population level and capturing the between-subject variability indexed by the probability value for each voxel to be identified as lying within the locus coeruleus (Fig. 3B). As a measure of locus coeruleus integrity, we quantified contrast by calculating the contrast-to-noise ratio (CNR) with respect to a reference region in the central pons (Fig. 3B). A CNR map was computed voxel-by-voxel on the average MT image for each subject using the signal difference between a given voxel and the mean intensity in the reference region ($Mean_{REF}$) divided by the SD (SD_{REF}) of the reference signals

$$CNR = \frac{v - Mean_{REF}}{SD_{REF}} \quad (1)$$

CNR values were computed bilaterally on the CNR map by applying the independent locus coeruleus probabilistic atlas (thresholded at 5% probability across all locus coeruleus voxels to improve sensitivity). To obtain summary indices of CNR for subsequent analyses, we extracted mean CNR values for the rostral, middle and caudal portions of the LC (defined by splitting the atlas into three equal numbers of z slices as previously shown; O'Callaghan et al., 2021; Fig. 3C), collapsing across the left and right locus coeruleus.

Voxel-based morphometry estimates of gray matter volume for rIFG and preSMA cortical areas were extracted from functionally-defined masks previously defined by Tsvetanov et al. (2018). For the fMRI SST-

related functional connectivity, we used psychophysiological interaction measures between rIFG and preSMA as estimated by Tsvetanov et al. (2018). Specifically, group independent components analysis (ICA) decomposed the fMRI signal into functional components that were activated in the contrast successful stop $>$ unsuccessful stop. Then correlational psychophysiological interactions analysis was used to estimate patterns of functional connectivity modulation between rIFG and preSMA. The resulting measure quantifies differences in connectivity (i.e., modulation) between successful and unsuccessful action cancellation trials within the rIFG-preSMA network (for further details, see Tsvetanov et al., 2018).

Analyses

To infer the latency of the unobservable response inhibition (i.e., the SSRT) we adopted hierarchical Bayesian estimation of a parametric race model of the SST (Matzke et al., 2013). Accordingly, performance on the SST is modeled as a race between three independent processes: one corresponding to the stop process, and two corresponding to go processes that match or mismatch the go stimulus. Successful response inhibition in stop-signal trials occurs when the stop process finishes its race before both go processes. Correct responses on go trials, instead, require the matching go process to finish its race before the mismatching go process. The finish time distribution of the stop process is inferred by estimating the RT distribution of unsuccessful stop trials (i.e., signal respond RTs; for details, see Matzke et al., 2013). The model assumes that the finish times of the stop and go processes follow an ex-Gaussian distribution (Heathcote et al., 2019). Thus, for each process, we described the corresponding ex-Gaussian distribution by estimating the mean μ and SD σ of its Gaussian component, and the mean (i.e., inverse rate) τ of its exponential component.

Further, we estimated the probability that the stop and go processes failed to start, referred to as “trigger failure” and “go failure” (Matzke et al., 2019). These attentional failures can be common in the SST and, if not accounted for, bias estimation of the stop process (Matzke et al., 2019). Before fitting the model, we excluded implausibly fast (<0.25 s) RTs, as well as outliers go RTs exceeding ± 2.5 SDs from the participant's mean (Matzke, et al., 2013; O'Callaghan et al., 2021).

We estimated the posterior distributions of the parameters using Markov Chain Monte Carlo (MCMC) sampling. The parameters were estimated hierarchically, such that parameters for a given participant are assumed to be drawn from corresponding group-level normal distributions. We adopted prior distributions identical to those suggested by the model developers (Heathcote et al., 2019), except for slightly higher prior mean values for $\mu_{go-match}$ (1.5 s), $\mu_{go-mismatch}$ (1.5 s), and μ_{stop} (1 s), to account for slower RT in older age (O'Callaghan et al., 2021). MCMC sampling initially ran with 33 chains (i.e., three times the number of parameters), with thinning of every 10th sample and a 5% probability of

migration. Visual inspection of the MCMC chains as well as the potential scale reduction statistic \hat{R} (<1.1 for all parameters; mean \hat{R} across subjects mean \pm SD: 1.009 ± 0.002) were used to assess model fit convergence. After confirming convergence, an additional 500 iterations for each chain were run to obtain a posterior distribution for each parameter. The model's goodness of fit was confirmed by comparing the observed data to simulated data generated from the model's posterior predictive distribution (Fig. 2C).

The SSRT was the primary outcome of interest, computed as the mean of the ex-Gaussian finish time distribution of the stop process, which is given by $\mu_{\text{stop}} + \tau_{\text{stop}}$. We repeated this computation for each MCMC sample to approximate a posterior distribution of SSRT. The same approach was adopted to draw a posterior distribution of go RT ($\mu_{\text{go-match}} + \tau_{\text{go-match}}$).

We used the statistical software package R (<http://www.r-project.org/>), following our preregistered analysis plan (<https://osf.io/zgj9n/>). For primary analyses we used Bayesian statistics which enables to quantify evidence in favor of the alternate hypothesis as well as evidence for the null hypothesis (of an absence of effect). We quantify relative evidence through Bayes factors (BFs) and for their interpretation we adhere to consensus guidelines (Jeffreys, 1961). For completeness, we also present classical frequentist analyses with $\alpha = 0.05$ criterion for significance and report η^2 as a measure of effect-size for all the regression analyses.

For all the regression analyses, we included sex as a binary covariate to account for possible sex-related differences in locus coeruleus signal (Clewett et al., 2016). We additionally controlled for changes in gray matter volume of the rIFG and preSMA, and check that regression assumptions are met. To control for age-related overall cortical shrinkage, we undertook an additional analysis, as an exploratory departure from the preregistration, in which we regressed the volumetric values of rIFG and preSMA against each individual's total gray matter volumes and used the residuals as predictors. The results were equivalent to those of the original preregistered analyses. We include age as a continuous moderator to take into account possible age-related changes in the reliance of response inhibition on both locus coeruleus integrity and connectivity (Tsvetanov et al., 2018). To prevent collinearity issues, the continuous variables forming the interaction term of regression were mean centered. Moreover, since we are focusing on changes over and above the main effect of age on the locus coeruleus, locus coeruleus CNR values were regressed onto age and the residuals used as predictor.

For the moderated mediation analysis, the choice of the model structure was guided by a previous interventional study of the effect of atomoxetine on functional connectivity between preSMA and rIFG (Rae et al., 2016, see their Fig. 3a for a depiction of the model). The approach allows us to estimate the shared variance between locus coeruleus signal and functional connectivity. The model was tested using the PROCESS macro model 15 in R using a bootstrap approach (Preacher and Hayes, 2004). The moderated mediation model tests for locus coeruleus-induced variability in response inhibition (direct effect, path *c*), and in functional connectivity mediating the effect on response inhibition (mediated effect, path *ab*). The model also tests whether the direct and indirect (i.e., mediated) effects of locus coeruleus on response inhibition change with age (age moderation, paths *b2* and *c2*).

Software and equipment

The ex-Gaussian model fitting was performed with the Dynamic Models of Choice toolbox (Heathcote et al., 2019), implemented in R (version 4.0, R Core Team, 2019). Further statistical analyses in R used the 'tidyverse' (Wickham et al., 2019) for data organization and visualization, 'processR' with 'lavaan' (Rosseel, 2012) packages for path analysis, and the 'BayesFactor' (Morey et al., 2018) and 'bayestestR' (Makowski et al., 2019) packages for BF analysis.

Results

We confirmed the task performance expectations in that (1) the group SSRT (median 161 ms) and Go reaction times (median 593 ms) were within the range expected from the literature on

related tasks, as show in Figure 2B; (2) commissions error latencies were shorter than accurate Go reaction times, indicative of impulsive responses (Fig. 2C); and (3) errors and latencies were approximately equal between left-hand and right-hand responses (Fig. 2C). The Stop signal algorithm converged on average 57.4% accuracy (SD 12.8%), and there was no evidence for an effect of age of the participants on accuracy levels of the staircase procedure (linear regression, $\text{BF}_{\text{H1}} = 0.85$, $p = 0.095$). In the following sections, we relate individual differences in performance to locus coeruleus CNR, using the 5% atlas (i.e., including voxels with $\geq 5\%$ probability to be identified as belonging to the locus coeruleus), but note that results are qualitatively similar using the more conservative atlas threshold of 25%.

Locus coeruleus integrity predicts individual differences in response inhibition

We tested for effects of locus coeruleus integrity (as CNR) on response inhibition (the SSRT) using multiple linear regression (Fig. 4A). The locus coeruleus integrity was associated with faster inhibitory responses but the strength of such association diminishes with age (interaction LC CNR \times age: $\text{BF}_{\text{H1}} = 16.866$; $t_{(55)} = 2.793$; $p = 0.007$; $\eta^2 = 0.11$; Fig. 4B). This moderation remains significant even after controlling for loss of gray matter in preSMA and rIFG regions, crucial components of the stopping-network ($\text{BF}_{\text{H1}} = 11.9$; $t_{(55)} = 2.871$; $p = 0.006$; $\eta^2 = 0.12$). No evidence was found for an effect of sex ($\text{BF}_{\text{H1}} = 0.473$; $t_{(55)} = -0.983$; $p = 0.329$; $\eta^2 = 0.03$) nor for volumetric differences in the preSMA ($\text{BF}_{\text{H1}} = 0.660$; $t_{(55)} = -0.782$; $p = 0.437$; $\eta^2 < 0.01$) and rIFG ($\text{BF}_{\text{H1}} = 0.606$; $t_{(55)} = -0.374$; $p = 0.71$; $\eta^2 = 0.02$) across subjects. To confirm that the parameter estimates of the multiple linear regression were not driven by the excessive influence of any given participant, we calculated Cook's distance which quantifies the influence of each data point on all parameters of the linear model simultaneously. As a rule of thumb, a participant is deemed overly influential if their Cook's distance exceeds four divided by the total number of participants (Van der Meer et al., 2010). In our sample, the Cook's distance values ranged from 0 to 0.063, within the applicable cutoff value of $4/62 = 0.064$. In a further effort to ensure robustness of our results, we re-fit the model using robust linear regression, which is less sensitive to data outliers than the conventional ordinary least squares method. The results of the robust analysis confirmed the results from the conventional linear regression showing a significant locus coeruleus integrity \times age interaction ($t_{(55)} = 3.006$; $p = 0.0038$), but no significant main effects of sex ($t_{(55)} = -0.899$; $p = 0.371$) or gray volume in preSMA ($t_{(55)} = -0.802$; $p = 0.42$) and rIFG ($t_{(55)} = -0.498$; $p = 0.618$).

The observed moderating effect of age on the association of locus coeruleus integrity with inhibitory control might be confounded by differences in the degree to which a participant has "successfully aged" cognitively and maintained cognitive ability on par with early adult life in contrast to "unsuccessfully aged" cognitively with decline in cognitive ability. To estimate this change in cognitive ability, one can compare current fluid intelligence to crystallized intelligence. This difference (ability discrepancy score) approximates the degree to which a participant has sustained or changed their cognitive ability, with lower fluid than crystallized intelligence as a marker of "unsuccessful aging" (McDonough et al., 2016). We tested for a possible role of unsuccessful aging by including ability discrepancy in the interaction term locus coeruleus CNR \times age, while controlling for sex and cortical volumetric changes. Bayesian analysis confirmed the age-moderated relationship between locus coeruleus CNR and

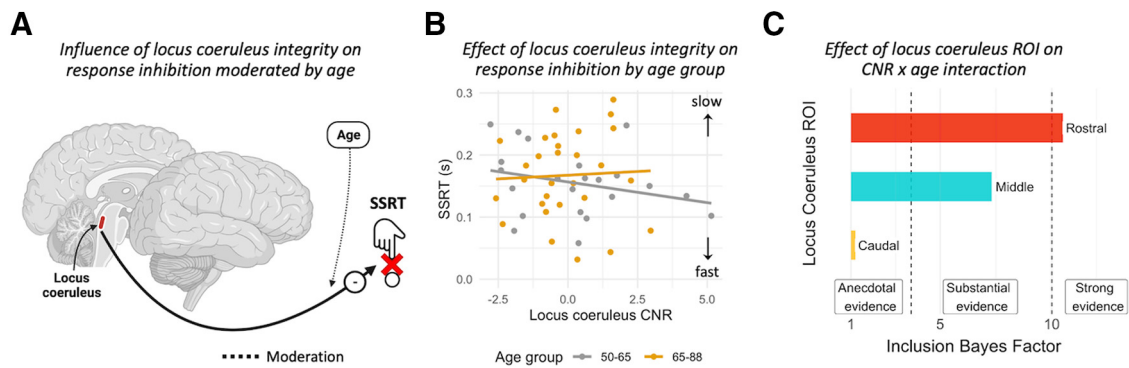


Figure 4. *A, B*, SSRT estimates as a function of age adjusted locus coeruleus CNR and age group. The interaction with age is estimated as a continuous variable (see text) but binarized for visualization purposes only. *C*, Bayesian evidence for an association between the integrity of rostral, and caudal subregions of the locus coeruleus with response inhibition.

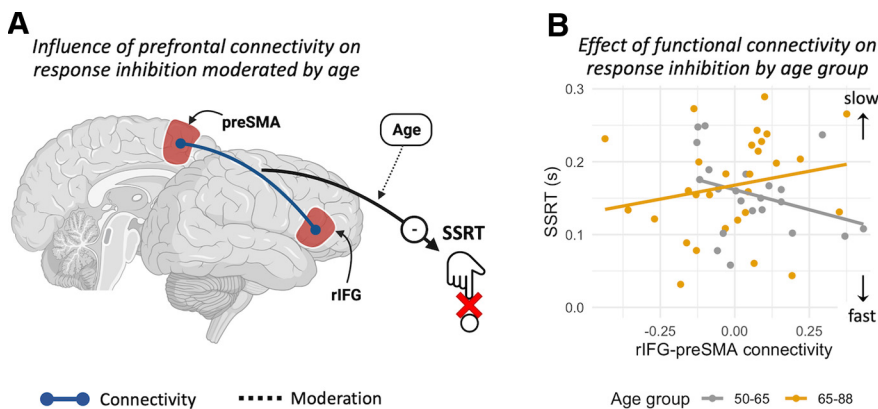


Figure 5. *A*, Age moderates the influence of connectivity between the preSMA and rIFG on response inhibition (SSRT). *B*, SSRT estimates as a function of connectivity between preSMA and rIFG. The interaction with age is estimated as a continuous variable (see text) but binarized for visualization purposes only.

response inhibition observed in the previous analyses ($BF_{H1} = 8.15$; although not significant with frequentist analysis $t_{(51)} = 1.326$; $p = 0.19$; $\eta^2 = 0.08$). However, there was no evidence in support for a role of ability discrepancy ($BF_{H1} = 0.434$; $t_{(51)} = -0.467$; $p = 0.642$; $\eta^2 < 0.01$), nor for interaction effects of ability discrepancy \times age ($BF_{H1} = 0.500$; $t_{(51)} = 0.162$; $p = 0.871$; $\eta^2 < 0.01$), or for the interaction CNR \times ability discrepancy ($BF_{H1} = 0.835$; $t_{(51)} = 1.041$; $p = 0.302$; $\eta^2 = 0.05$), and only anecdotal evidence for the interaction CNR \times ability discrepancy \times age ($BF_{H1} = 2.25$; $t_{(51)} = 2.215$; $p = 0.031$; $\eta^2 = 0.07$). Therefore, age affects the modulatory effect of locus coeruleus integrity on response inhibition regardless of individuals' lifetime decline in cognitive ability.

To probe the specificity of the relationship between locus coeruleus integrity and action cancellation, we repeated the linear regression analysis replacing SSRTs with successful Go reaction times as outcome. There was strong evidence for slowing of Go reaction times with age ($BF_{H1} = 13.11$; $t_{(55)} = 2.972$; $p = 0.0043$; $\eta^2 = 0.13$) but no evidence for a link between Go reactions times and locus coeruleus integrity (main effect CNR: $BF_{H1} = 0.341$; $t_{(55)} = 0.517$; $p = 0.607$; $\eta^2 < 0.01$; interaction CNR \times age: $BF_{H1} = 0.693$; $t_{(55)} = 1.083$; $p = 0.283$; $\eta^2 = 0.02$).

Integrity of the rostral subregion of the locus coeruleus is associated with response inhibition

Subregions of the locus coeruleus may have differential associations to cognition, behavior and pathology given the

heterogeneity in its topographic organization. Here, we estimated the association between the integrity of subregions of the locus coeruleus with response inhibition. In the preregistered analysis plan, we proposed to fit a multiple linear regression model including the interaction between rostral, middle, caudal subregions of the locus coeruleus and age while controlling for sex and gray matter volume as in our previous analyses. However, diagnostic tests indicated a strong multicollinearity in the interaction term driven by the middle CNR (variance inflation factor > 10). We therefore deviate from the preregistered plan for this test and performed a Bayesian model comparison to assess which subregions was driving observed locus coeruleus CNR \times age interaction.

We compared three linear models including the interaction term CNR \times age (one model for each subregion) to a simpler specific null model where the influence of the CNR \times age interaction was not included (i.e., the regressor coefficient for the interaction was assumed to be set to zero). Bayesian factors compare these models. The model comparison results provide strong evidence ($BF_{H1} = 10.53$) in support of the model including the rostral CNR \times age interaction, substantial evidence for the model including middle CNR \times age interaction ($BF_{H1} = 7.29$), and only anecdotal evidence for the model with caudal CNR \times age interaction ($BF_{H1} = 1.16$; Fig. 4C). Thus, our results provide corroborating evidence that the Rostral subregion drives the interaction between locus coeruleus CNR and age. Milder effects are observed for the middle portion of the locus coeruleus. A possible explanation for the anecdotal evidence in the caudal portion, is that this part of the locus coeruleus has high intersubjective variability and partial volume effects (Ye et al., 2021b). Therefore, we went beyond the preregistered analysis to compare the signal-to-noise ratio (SNR) among subregions. There was anecdotal evidence for a lack of difference in SNR between the caudal portion ($M = 40.7$, $SD = 12$) and middle ($M = 38.5$, $SD = 6.7$; $BF_{H1} = 0.379$, $t_{(62)} = 1.399$, $p = 0.501$, $CI [-0.981; 5.559]$) or rostral ($M = 43.9$, $SD = 9.09$; $BF_{H1} = 0.686$, $t_{(62)} = -1.639$, $p = 0.318$, $CI [-6.301; 0.624]$) portions. The apparent differential contribution of rostral versus caudal locus coeruleus integrity to inhibitory control is therefore not likely to be because of differential SNR.

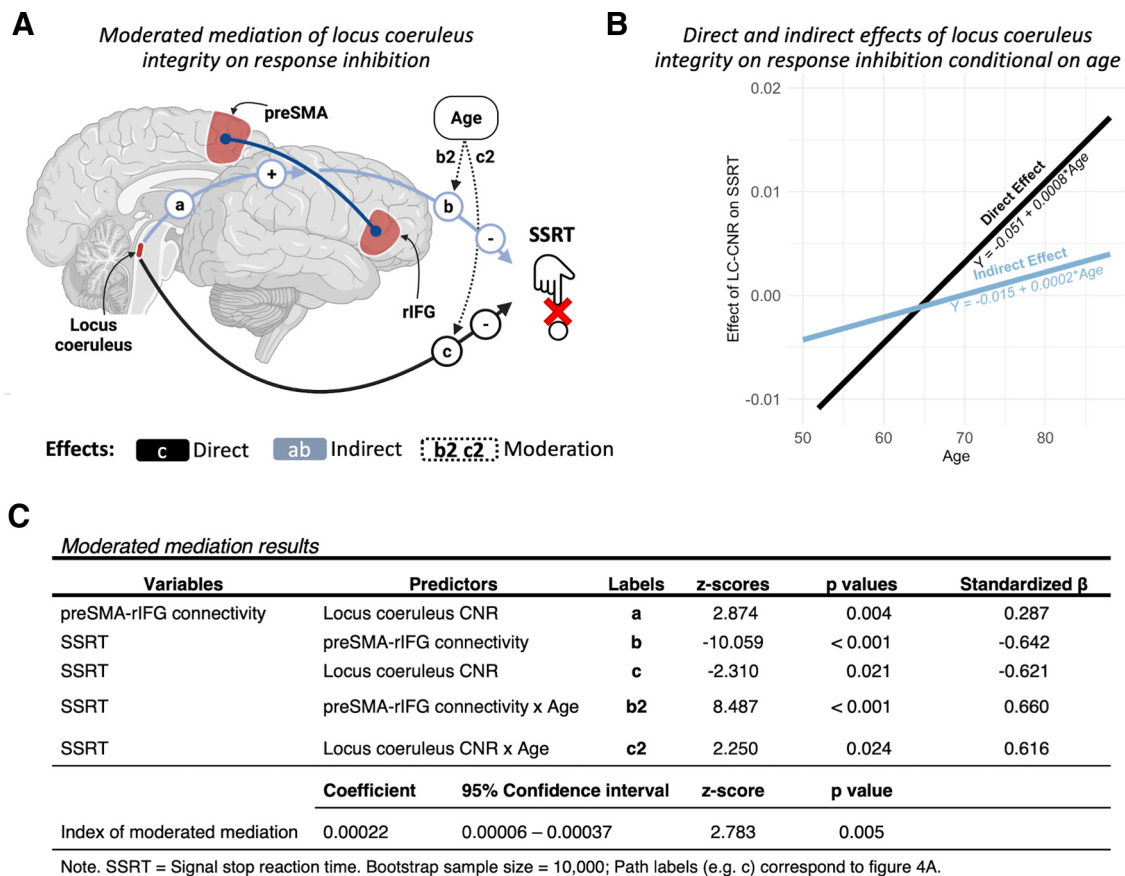


Figure 6. *A*, Moderated mediation model, with locus coeruleus integrity as a predictor (LC-CNR), functional connectivity within the prefrontal stopping-network as a mediator (connectivity), and SSRTs as an outcome. Age was included as a second-level moderator. *B*, Direct and indirect (i.e., mediated by functional connectivity) effects of locus coeruleus integrity on response inhibition, conditional on age. *C*, Results from the moderated mediation. Labels match with those identifying the model's paths on panel *A*.

Modulation of connectivity between preSMA and rIFG predicts individual differences in response inhibition

We tested whether the performance related connectivity (between successful and unsuccessful stop trials) within the prefrontal stopping-network was related to individual differences in response inhibition (SSRT), using multiple linear regression. Substantial evidence indicates that Age moderated the relationship between preSMA-rIFG connectivity and response inhibition ($BF_{HI} = 5.12$; $t_{(55)} = 2.354$; $p = 0.022$; $\eta^2 = 0.08$; Fig. 5B) qualitatively similar to the effect observed when locus coeruleus CNR was used as predictor. There was no evidence for an effect of sex ($BF_{HI} = 0.494$; $t_{(55)} = -1.05$; $p = 0.289$; $\eta^2 = 0.03$) or volumetric gray matter differences in preSMA ($BF_{HI} = 0.555$; $t_{(55)} = -0.482$; $p = 0.631$; $\eta^2 < 0.01$) and rIFG regions ($BF_{HI} = 0.536$; $t_{(55)} = -0.252$; $p = 0.801$; $\eta^2 = 0.02$). We confirmed robustness of our linear regression results by examining the Cook's distance of each participant (range 0–0.058, below the 0.064 threshold) as well as by showing that results were qualitatively identical when re-fitting the data with a robust regression approach. Specifically, the robust regression results confirm a significant Connectivity \times Age interaction ($t_{(55)} = 2.828$; $p = 0.006$) but no significant main effects for sex ($t_{(55)} = -0.709$; $p = 0.481$) or gray matter volume in preSMA ($t_{(55)} = -0.479$; $p = 0.625$) and rIFG ($t_{(55)} = -0.365$; $p = 0.853$).

Modulation of prefrontal connectivity partially mediates influence of locus coeruleus on response inhibition

Next, we tested whether task-related functional connectivity mediated the variance between locus coeruleus signal and SSRT,

subject to moderation by age (Fig. 6A). The direct association between locus coeruleus and response inhibition was moderated by age ($c2$: standardized $\beta = 0.616$; $p = 0.024$). The association between connectivity and response inhibition was also conditional on age ($b2$: standardized $\beta = 0.660$; $p < 0.0001$). A formal test of moderated mediation based on the index term (Hayes, 2015) indicated that the effect of locus coeruleus integrity on response inhibition was partly mediated by functional connectivity in the prefrontal stopping-network, but this relationship changed with age (ab : coefficient of moderated mediation = 0.00022; bootstrapped 95% CI [0.00006, 0.00037]; $p = 0.005$; proportion moderated = 0.45). The moderated direct and indirect effects of locus coeruleus integrity on response inhibition are depicted on Figure 6B.

Discussion

The principal results of this preregistered study are that (1) individual differences in stopping efficiency are related to the integrity of the locus coeruleus; and (2) this effect is partially mediated by the facilitation of connectivity within the prefrontal stopping-network. These effects were observed in healthy adults from a population-based cohort, but moderated by age, over and above the main effect of age on locus coeruleus integrity.

This behavioral effect is mainly associated with integrity of the rostral subregion of the locus coeruleus, which preferentially targets prefrontal cortex, and is affected by healthy aging (Mason and Fibiger, 1979; Loughlin et al., 1986). Crucially, these effects

were observed after correction for a possible main effect of age on the locus coeruleus. Nonetheless, the influence of locus coeruleus variability is moderated by age. Previous reports linked variation of rostral locus coeruleus intensity to cognitive performances in healthy subjects. Preserved integrity of the rostral locus coeruleus in healthy older adults has been associated with better cognitive function (Manaye, et al., 1995; Hämmerer et al., 2018; Dahl et al., 2019; Liu et al., 2020). Our results support this previous work and extend the evidence for an influence of the locus coeruleus noradrenaline system on inhibitory control.

The influence of noradrenaline may also be understood in terms of its effect on task-related connectivity between regions (Rae et al., 2016; Holland et al., 2021). For inhibitory control, connectivity between the rIFG and preSMA are of particular relevance: lesion studies, transient interference by magnetic or electrical stimulation, and neuroimaging work provide converging evidence that interactions between these regions are crucial for successful response inhibition (Chambers et al., 2006; Duann et al., 2009; Forstmann et al., 2012; Rae et al., 2015). We found that the effect of locus coeruleus integrity on response inhibition is partly mediated by changes in functional connectivity between the rIFG and preSMA. These findings reinforce previous reports on the effect of the noradrenaline reuptake inhibitor atomoxetine on response inhibition in Parkinson's disease. For example, Rae et al. (2016) observed that in patients, connectivity between of preSMA on the rIFG was reduced, but restored by atomoxetine. Using dynamic causal modeling, they showed that atomoxetine restored the effective connectivity between preSMA and rIFG, and increased the strength of their interacting projections to the subthalamic nucleus. Our results similarly associate increased connectivity between these two areas to enhanced response inhibition, and provide evidence that modulation within the stopping-network is related to the integrity of the locus coeruleus, the principal source of noradrenaline.

The influence of both locus coeruleus integrity and prefrontal stopping-network connectivity on inhibitory control changed with age. Our results confirmed such an interaction: higher age-adjusted integrity within the younger and middle age range (50–65 years) of healthy adults was associated with positive modulation of the stopping-network and better inhibitory control. This was not observed over 65 years.

Ageing is also associated with decline of other aspects of motor performance such as psychomotor slowing and reduced fine motor skills (Salthouse, 2000; Seidler et al., 2010). A contributor to age-related performance decline is loss of gray matter volume (Draganski et al., 2013) with evidence from functional neuroimaging studies for adaptive plasticity paralleling structural decline (Tsvetanov et al., 2021). Consequently, older adults may display more widespread brain activation, weaker segregation of local networks and weaker interhemispheric connectivity (Rowe et al., 2006; Chan et al., 2014; Geerligs et al., 2015; Tsvetanov et al., 2016). Evidence to date suggests that less segregated brain networks contribute to age-related decline in cognitive and sensorimotor performance (Chan et al., 2014; Geerligs et al., 2015; King et al., 2018; Bethlehem et al., 2020). Indeed, similarly to our results, analysis of cortical connectivity in the CamCAN dataset showed that stopping efficiency in older adults relied more strongly on connectivity than in their younger counterparts (Tsvetanov et al., 2018), in accord with preclinical studies of the effects of locus coeruleus plasticity and connectivity (Bear and

Singer, 1986; Coull et al., 1999; Martins and Froemke, 2015). Further longitudinal studies are warranted to investigate age-related changes in the way locus coeruleus integrity and cortical connectivity impact on inhibitory control.

Our preregistered analysis was designed to specifically probe the association of locus coeruleus integrity with response inhibition and differs in many respects from an earlier analysis of the Cam-CAN cohort looking for associations of coeruleus integrity with a cognitive component expressing mainly general abilities (Liu et al., 2020). We focused on adults aged above 50 years, for better estimation of structural integrity of the locus coeruleus using MT-weighted MRI. This is because of the greater neuromelanin based contrast with age (Zecca et al., 2004). The locus coeruleus signal was extracted through a probabilistic atlas-based segmentation, which provides unbiased estimation, with superior accuracy and reliability compared with the manual segmentation approaches (Chen et al., 2014; Langley et al., 2017; Ye et al., 2021a). These features are preferable when using 3T MRI images, where the manual segmentation approach may be unreliable because of the relatively low SNR. Next, the SSRT was estimated using a Bayesian parametric model of the SST which isolates attentional confounds from response inhibition (Matzke et al., 2013). These differences between studies might explain the fact that no effect of locus coeruleus signal on the SST was observed by Liu et al. (2020).

There are limitations in the current study that should be considered when interpreting the results and need to be addressed in future studies. First, the focus on ages above 50 years reduced sample size. Power calculations confirmed that our study was well powered for the intended analyses (see preregistration, <https://osf.io/zgj9n/>). However, individual variability in locus coeruleus signal increases with age (Liu et al., 2019; Ye et al., 2021b). Second, our results are based on a cross-sectional cohort. Therefore, our conclusions merely speak to the effects of age and its correlates, as assessed across individuals, but provide no insight on the dynamic process of individual aging. A larger sample size including more subjects of advanced age or a longitudinal cohort might be needed in future studies to confirm the impact of aging on the relationship between locus coeruleus and inhibitory control. Third, participants' cognitive functions were screened with the ACE-R test which may lack the sensitivity to detect latent Alzheimer's disease pathology in the older group. Notably, the regional vulnerability of locus coeruleus neurons varies between disorders and the rostral region, which we show being related to response inhibition, is especially vulnerable to Alzheimer's disease and latent pathology with healthy aging (Mason and Fibiger, 1979; German et al., 1992). Fourth, the 3T MRI images used in the present study afford a lower SNR compared with 7T scans. However, the resulting reduced sensitivity would be expected to increase Type II but not Type I error. Finally, the present work focused on the modulatory role of the locus coeruleus noradrenergic system on action cancellation. We acknowledge that other neuromodulators, such as serotonin, can play a crucial role in regulating forms of inhibitory control other than action cancellation (Cools et al., 2008; Eagle et al., 2008; Ye et al., 2014; Hughes et al., 2015).

In conclusion, we show that the ability to inhibit responses relies on both the locus coeruleus and its facilitation of connectivity within the prefrontal cortex. The locus coeruleus integrity has different implications for inhibitory control at different ages. These findings contribute to the broader understanding of the importance of noradrenergic systems for executive functions in

normal populations, with implications for impulsive clinical disorders.

References

- Aston-Jones G, Cohen JD (2005) An integrative theory of locus coeruleus-norepinephrine function: adaptive gain and optimal performance. *Annu Rev Neurosci* 28:403–450.
- Bari A, Mar AC, Theobald DE, Elands SA, Oganya KCNA, Eagle DM, Robbins TW (2011) Prefrontal and monoaminergic contributions to stop-signal task performance in rats. *J Neurosci* 31:9254–9263.
- Bear MF, Singer W (1986) Modulation of visual cortical plasticity by acetylcholine and noradrenaline. *Nature* 320:172–176.
- Bethlehem RAI, Paquola C, Seidlitz J, Ronan L, Bernhardt B, Consortium CC, Tsvetanov KA (2020) Dispersion of functional gradients across the adult lifespan. *Neuroimage* 222:117299.
- Betts MJ, Cardenas-Blanco A, Kanowski M, Jessen F, Düzel E (2017) In vivo MRI assessment of the human locus coeruleus along its rostrocaudal extent in young and older adults. *Neuroimage* 163:150–159.
- Bouret S, Sara SJ (2005) Network reset: a simplified overarching theory of locus coeruleus noradrenaline function. *Trends Neurosci* 28:574–582.
- Chamberlain SR, Müller U, Blackwell AD, Clark L, Robbins TW, Sahakian BJ (2006) Neurochemical modulation of response inhibition and probabilistic learning in humans. *Science* 311:861–863.
- Chamberlain SR, Hampshire A, Müller U, Rubia K, Del Campo N, Craig K, Regenthal R, Suckling J, Roiser JP, Grant JE, Bullmore ET, Robbins TW, Sahakian BJ (2009) Atomoxetine modulates right inferior frontal activation during inhibitory control: a pharmacological functional magnetic resonance imaging study. *Biol Psychiatry* 65:550–555.
- Chambers CD, Bellgrove MA, Stokes MG, Henderson TR, Garavan H, Robertson IH, Morris AP, Mattingley JB (2006) Executive “brake failure” following deactivation of human frontal lobe. *J Cogn Neurosci* 18:444–455.
- Chan MY, Park DC, Savalia NK, Petersen SE, Wig GS (2014) Decreased segregation of brain systems across the healthy adult lifespan. *Proc Natl Acad Sci U S A* 111:E4997–E5006.
- Chen X, Huddleston DE, Langley J, Ahn S, Barnum CJ, Factor SA, Levey AI, Hu X (2014) Simultaneous imaging of locus coeruleus and substantia nigra with a quantitative neuromelanin MRI approach. *Magn Reson Imaging* 32:1301–1306.
- Clewett DV, Lee TH, Greening S, Ponzio A, Margalit E, Mather M (2016) Neuromelanin marks the spot: identifying a locus coeruleus biomarker of cognitive reserve in healthy aging. *Neurobiol Aging* 37:117–126.
- Coull JT, Büchel C, Friston KJ, Frith CD (1999) Noradrenergically mediated plasticity in a human attentional neuronal network. *Neuroimage* 10:705–715.
- Cools R, Roberts AC, Robbins TW (2008) Serotonergic regulation of emotional and behavioural control processes. *Trends Cogn Sci* 12:31–40.
- Dahl M, Mather M, Düzel S, Bodammer NC, Lindenberger U, Kühn S, Werkle-Bergner M (2019) Rostral locus coeruleus integrity is associated with better memory performance in older adults. *Nat Hum Behav* 3:1203–1214.
- Dayan P, Yu AJ (2006) Phasic norepinephrine: a neural interrupt signal for unexpected events. *Network* 17:335–350.
- Draganski B, Lutti A, Kherif F (2013) Impact of brain aging and neurodegeneration on cognition. *Curr Opin Neurol* 26:640–645.
- Duann JR, Ide JS, Luo X, Li CSR (2009) Functional connectivity delineates distinct roles of the inferior frontal cortex and presupplementary motor area in stop signal inhibition. *J Neurosci* 29:10171–10179.
- Eagle DM, Baunez C (2010) Is there an inhibitory-response-control system in the rat? Evidence from anatomical and pharmacological studies of behavioral inhibition. *Neurosci Biobehav Rev* 34:50–72.
- Eagle DM, Bari A, Robbins TW (2008) The neuropsychopharmacology of action inhibition: cross-species translation of the stop-signal and go/no-go tasks. *Psychopharmacology (Berl)* 199:439–456.
- Friston KJ, Büchel C, Fink GR, Morris J, Rolls E, Dolan RJ (1997) Psychophysiological and modulatory interactions in neuroimaging. *Neuroimage* 6:218–229.
- Forstmann BU, Keuken MC, Jahfari S, Bazin P-L, Neumann J, Schäfer A, Anwander A, Turner R (2012) Cortico-subthalamic white matter tract strength predicts interindividual efficacy in stopping a motor response. *Neuroimage* 60:370–375.
- Geerligns L, Renken RJ, Saliassi E, Maurits NM, Lorist MM (2015) A brain-wide study of age-related changes in functional connectivity. *Cereb Cortex* 25:1987–1999.
- German DC, Manaye KF, White CL, Woodward DJ, McIntire DD, Smith WK, Kalaria RN, Mann DM (1992) Disease-specific patterns of locus coeruleus cell loss. *Ann Neurol* 32:667–676.
- Hämmerer D, Callaghan MF, Hopkins A, Kosciessa J, Betts M, Cardenas-Blanco A, Kanowski M, Weiskopf N, Dayan P, Dolan RJ, Düzel E (2018) Locus coeruleus integrity in old age is selectively related to memories linked with salient negative events. *Proc Natl Acad Sci U S A* 115:2228–2233.
- Hayes AF (2015) An index and test of linear moderated mediation. *Multivariate Behav Res* 50:1–22.
- Heathcote A, Lin YS, Reynolds A, Strickland L, Gretton M, Matzke D (2019) Dynamic models of choice. *Behav Res Methods* 51:961–985.
- Holland N, Robbins TW, Rowe JB (2021) The role of noradrenaline in cognition and cognitive disorders. *Brain* 144:2243–2256.
- Hughes LE, Rittman T, Regenthal R, Robbins TW, Rowe JB (2015) Improving response inhibition systems in frontotemporal dementia with citalopram. *Brain* 138:1961–1975.
- Jeffreys H (1961) *Theory of probability*. Oxford: Clarendon Press.
- King BR, van Ruitenbeek P, Leunissen I, Cuyppers K, Heise KF, Santos Monteiro T, Hermans L, Levin O, Albouy G, Mantini D, Swinnen SP (2018) Age-related declines in motor performance are associated with decreased segregation of large-scale resting state brain networks. *Cereb Cortex* 28:4390–4402.
- Langley J, Huddleston DE, Liu CJ, Hu X (2017) Reproducibility of locus coeruleus and substantia nigra imaging with neuromelanin sensitive MRI. *MAGMA* 30:121–125.
- Liu KY, Acosta-Cabronero J, Cardenas-Blanco A, Loane C, Berry AJ, Betts MJ, Kievit RA, Henson RN, Düzel E, Howard R, Hämmerer D; Cam-CAN (2019) In vivo visualization of age-related differences in the locus coeruleus. *Neurobiol Aging* 74:101–111.
- Liu KY, Kievit RA, Tsvetanov KA, Betts MJ, Düzel E, Rowe JB, Howard R, Hämmerer D; Cam-CAN (2020) Noradrenergic-dependent functions are associated with age-related locus coeruleus signal intensity differences. *Nat Commun* 11:1712.
- Loughlin SE, Foote SL, Bloom FE (1986) Efferent projections of nucleus locus coeruleus: topographic organization of cells of origin demonstrated by three-dimensional reconstruction. *Neuroscience* 18:291–306.
- Makowski D, Ben-Shachar M, Lüdtke D (2019) bayestestR: describing effects and their uncertainty, existence and significance within the Bayesian framework. *J Open Source Soft* 4:1541.
- Martins AR, Froemke RC (2015) Coordinated forms of noradrenergic plasticity in the locus coeruleus and primary auditory cortex. *Nat Neurosci* 18:1483–1492.
- Manaye KF, McIntire DD, Mann DMA, German DC (1995) Locus coeruleus cell loss in the aging human brain: a non-random process. *J Comp Neurol* 358:79–87.
- Mason ST, Fibiger HC (1979) Regional topography within noradrenergic locus coeruleus as revealed by retrograde transport of horseradish peroxidase. *J Comp Neurol* 187:703–724.
- Matzke D, Dolan CV, Logan GD, Brown SD, Wagenmakers EJ (2013) Bayesian parametric estimation of stop-signal reaction time distributions. *J Exp Psychol Gen* 142:1047–1073.
- Matzke D, Curley S, Gong CQ, Heathcote A (2019) Inhibiting responses to difficult choices. *J Exp Psychol Gen* 148:124–142.
- McDonough IM, Bischof GN, Kennedy KM, Rodrigue KM, Farrell ME, Park DC (2016) Discrepancies between fluid and crystallized ability in healthy adults: a behavioral marker of preclinical Alzheimer’s disease. *Neurobiol Aging* 46:68–75.
- Morey R, Rouder JN, Jamil T, Urbanek S, Forner K, Ly A (2018) Package BayesFactor 0.9.12–4.2.
- O’Callaghan C, Hezemans FH, Ye R, Rua C, Jones PS, Murley AG, Holland N, Regenthal R, Tsvetanov KA, Wolpe N, Barker RA, Williams-Gray CH, Robbins TW, Passamonti L, Rowe JB (2021) Locus coeruleus integrity and the effect of atomoxetine on response inhibition in Parkinson’s disease. *Brain* 144:2513–2526.
- Passamonti L, Lansdall CJ, Rowe JB (2018) The neuroanatomical and neurochemical basis of apathy and impulsivity in frontotemporal lobar degeneration. *Curr Opin Behav Sci* 22:14–20.

- Preacher KJ, Hayes AF (2004) SPSS and SAS procedures for estimating indirect effects in simple mediation models. *Behav Res Methods Instrum Comput* 36:717–731.
- Rae CL, Hughes LE, Anderson MC, Rowe JB (2015) The prefrontal cortex achieves inhibitory control by facilitating subcortical motor pathway connectivity. *J Neurosci* 35:786–794.
- Rae CL, Nombela C, Rodríguez PV, Ye Z, Hughes LE, Jones PS, Ham T, Rittman T, Coyle-Gilchrist I, Regenthal R, Sahakian BJ, Barker RA, Robbins TW, Rowe JB (2016) Atomoxetine restores the response inhibition network in Parkinson's disease. *Brain* 139:2235–2248.
- Rosseel Y (2012) lavaan: an R package for structural equation modeling. *J Stat Soft* 48:1–36.
- Rowe JB, Siebner H, Filipovic SR, Cordivari C, Gerschlager W, Rothwell J, Frackowiak R (2006) Aging is associated with contrasting changes in local and distant cortical connectivity in the human motor system. *Neuroimage* 32:747–760.
- Salthouse TA (2000) Aging and measures of processing speed. *Biol Psychol* 54:35–54.
- Seidler RD, Bernard JA, Burutolu TB, Fling BW, Gordon MT, Gwin JT, Kwak Y, Lipps DB (2010) Motor control and aging: links to age-related brain structural, functional, and biochemical effects. *Neurosci Biobehav Rev* 34:721–733.
- Shafto MA, Tyler LK, Dixon M, Taylor JR, Rowe JB, Cusack R, Calder AJ, Marslen-Wilson WD, Duncan J, Dalgleish T, Henson RN, Brayne C, Matthews FE; Cam-CAN (2014) The Cambridge Centre for ageing and neuroscience (cam-CAN) study protocol: a cross-sectional, lifespan, multidisciplinary examination of healthy cognitive ageing. *BMC Neurol* 14:204–225.
- Taylor JR, Williams N, Cusack R, Auer T, Shafto MA, Dixon M, Tyler LK, Cam-Can, Henson RN (2017) The Cambridge Centre for Ageing and Neuroscience (Cam-CAN) data repository: Structural and functional MRI, MEG, and cognitive data from a cross-sectional adult lifespan sample. *Neuroimage* 144:262–269.
- Tsvetanov KA, Henson RNA, Tyler LK, Razi A, Geerligs L, Ham TE, Rowe JB; Cambridge Centre for Ageing and Neuroscience (2016) Extrinsic and intrinsic brain network connectivity maintains cognition across the life-span despite accelerated decay of regional brain activation. *J Neurosci* 36:3115–3126.
- Tsvetanov KA, Ye Z, Hughes L, Samu D, Treder MS, Wolpe N, Tyler LK, Rowe JB; Cambridge Centre for Ageing and Neuroscience (2018) Activity and connectivity differences underlying inhibitory control across the adult life span. *J Neurosci* 38:7887–7900.
- Tsvetanov KA, et al. (2021) Brain functional network integrity sustains cognitive function despite atrophy in presymptomatic genetic frontotemporal dementia. *Alzheimers Dement* 17:500–514.
- Van der Meer T, Te Grotenhuis M, Pelzer B (2010) Influential cases in multi-level modeling: a methodological comment. *Am Sociol Rev* 75:173–178.
- Verbruggen F, et al. (2019) A consensus guide to capturing the ability to inhibit actions and impulsive behaviors in the stop-signal task. *Elife* 8:e46323.
- Watanabe T, Tan Z, Wang X, Martinez-Hernandez A, Frahm J (2019) Magnetic resonance imaging of noradrenergic neurons. *Brain Struct Funct* 224:1609–1625.
- Wickham H, et al. (2019) Welcome to the tidyverse. *J Open Source Softw* 4:1686.
- Ye Z, Altena E, Nombela C, Housden CR, Maxwell H, Rittman T, Huddleston C, Rae CL, Regenthal R, Sahakian BJ, Barker RA, Robbins TW, Rowe JB (2014) Selective serotonin reuptake inhibition modulates response inhibition in Parkinson's disease. *Brain* 137:1145–1155.
- Ye R, O'Callaghan C, Rua C, Hezemans FH, Holland N, Malpetti M, Jones, Passamonti L, Rowe J (2021a) 7T locus coeruleus imaging correlates of apathy and cognition in patients with Parkinson's disease and progressive supranuclear palsy. *Alzheimer's & Dementia* 18:1–3.
- Ye R, Rua C, O'Callaghan C, Jones PS, Hezemans FH, Kaalund SS, Tsvetanov KA, Rodgers CT, Williams G, Passamonti L, Rowe JB (2021b) An in vivo probabilistic atlas of the human locus coeruleus at ultra-high field. *Neuroimage* 225:117487.
- Zecca L, Youdim MBH, Riederer P, Connor JR, Crichton RR (2004) Iron, brain ageing and neurodegenerative disorders. *Nat Rev Neurosci* 5:863–873.